Ribosomal synthesis and folding of peptide-helical aromatic foldamer hybrids

Joseph M. Rogers [1,4], Sunbum Kwon [2,4], Simon J. Dawson[2], Pradeep K. Mandal [2], Hiroaki Suga [1]* and Ivan Huc [2,3]*

Translation, the mRNA-templated synthesis of peptides by the ribosome, can be manipulated to incorporate variants of the 20 cognate amino acids. Such approaches for expanding the range of chemical entities that can be produced by the ribosome may accelerate the discovery of molecules that can perform functions for which poorly folded, short peptidic sequences are ill suited. Here, we show that the ribosome tolerates some artificial helical aromatic oligomers, so-called foldamers. Using a flexible tRNA-acylation ribozyme—flexizyme—foldamers were attached to tRNA, and the resulting acylated tRNAs were delivered to the ribosome to initiate the synthesis of non-cyclic and cyclic foldamer–peptide hybrid molecules. Passing through the ribosome exit tunnel requires the foldamers to unfold. Yet foldamers encode sufficient folding information to influence the peptide structure once translation is completed. We also show that in cyclic hybrids, the foldamer portion can fold into a helix and force the peptide segment to adopt a constrained and stretched conformation.

In peptide biosynthesis, the ribosome, a large ribonucleoprotein complex[1], progresses along an mRNA template and brings together a succession of adapter tRNAs whose 3′-end hydroxyl groups are acylated with cognate amino acids. Three nucleotides of each tRNA (anticodon) match a given set of three nucleotides on the mRNA (codon), and one amino acid is delivered to the growing peptide chain. The nascent peptide emerges out of the so-called ribosome exit tunnel. Specific aminoacylation of tRNAs, catalysed by the corresponding aminoacyl–tRNA synthetases, dictates codons' assignment and constitutes the genetic code. Several methods have been developed to artificially expand[2–4] or reprogram[5,6] the genetic code by attaching non-proteinogenic amino acids to tRNAs. For example, versatile tRNA-acylation ribozymes, known as flexizymes[5], conveniently catalyse such attachments. Non-proteinogenic aminoacyl–tRNAs prepared by flexizymes can be added to solutions containing the translation-associating proteins, cofactors and ribosomes required for in vitro translation[7], allowing for the incorporation of a variety of synthetic building blocks[5] and expanding the chemical register of mRNA-encoded peptides[8].

Genetic code reprogramming has also revealed the tolerance of the ribosomal machinery to non-proteinogenic amino acids: α-amino acids bearing non-natural side chains[5], many D-amino acids[9,10] and even some β-amino acids[11] have been incorporated within peptidic sequences. Furthermore, chemistry that permits cyclization[12], as well as ester and N-alkylated amide functions[13,14], have been shown to be accepted by the ribosome. In addition to single amino acids, preformed di-, tri- or penta-peptides[15] and other organic building blocks[16] have also been attached directly to tRNA$^{fMet}_{CAU}$, the tRNA that initiates peptide synthesis by matching the start AUG codon of mRNA, and have been incorporated as small appendages at the N terminus of the translated peptide. These developments open up the prospect of hijacking the ribosome machinery to produce mRNA-encoded chemical entities ever more remote from α-peptides, with the notable advantages that (1) mRNA encoding gives access to sequence randomization and

selection from libraries containing trillions of unique sequences[17], and (2) enriching chemical diversity increases the range of accessible functions, including resistance to proteolytic degradation, cell penetration capabilities or protein recognition through the folding of short sequences. The stakes are thus high. However, beyond the key steps that have already been made[5,9–11,15–18], it is not yet known where definite limitations lie in this endeavour.

In the following, we present our discovery that the ribosome accepts objects far larger, and more distinct from peptides, than those previously considered. Specifically, we show that helical aromatic foldamers[19] (helically folded oligomeric backbones with aryl rings in their main chain) larger than 900 Da can be incorporated at the N terminus of a translated peptide or protein. In the resulting foldamer–peptide hybrids, the peptide component may represent less than half of the whole entity. The process was found to require foldamer unfolding to pass the exit tunnel. Yet, the folding propensity of these foldamers largely exceeds that of short peptides, and their incorporation amounts to encoding additional folding information that can effectively bias the peptide structure. For example, we show that macrocycles can be translated by the ribosome, whereby a foldamer segment adopts a helical conformation and forces a peptide segment to remain extended. Reciprocally, the peptide segment controls the handedness of the foldamer helix. These results expand the scope of ribosomal expression of mRNA-encoded non-natural sequences, and also introduce the benefits of using the stable conformations of foldamers to control peptide conformation.

Results and discussion

Our initial motivation stemmed from the consideration that short peptides are inherently flexible and not prone to folding, whereas some aromatic foldamers feature outstanding conformational stability and might thus serve as structural templates to assist peptide folding. Several approaches already exist to stabilize peptide conformation, including, but not limited to, the use of non-natural building blocks such as β-amino acids[20] or turn mimics[21], as well as

[1]Department of Chemistry, Graduate School of Science, The University of Tokyo, Tokyo, Japan. [2]CBMN Laboratory, Univ. Bordeaux, CNRS, IPB, Institut Européen de Chimie et Biologie, Pessac, France. [3]Present address: Department of Pharmacy, Ludwig-Maximilians-Universität, München, Germany. [4]These authors contributed equally: Joseph M. Rogers, Sunbum Kwon. *e-mail: hsuga@chem.s.u-tokyo.ac.jp; ivan.huc@cup.lmu.de

Fig. 1 | Aromatic oligoamide foldamers and their initiation of in vitro translation. a, Quinoline-based (**Q**) and pyridine-based (**P**) monomers with backbone (shown in bold) comparable to that of a dipeptide (Gly–Gly). **Q** can be functionalized with a variety of side chains (R). **b**, Intramolecular hydrogen bonds (dashed lines) within $\mathbf{Q}_n$ oligomers, together with aromatic stacking, allow for the formation of stable helices, as shown by the crystal structure of $\mathbf{Q}_{10}$ (right, side chains are omitted for clarity)[48]. **c**, Schematic representation of the acylation of tRNAs with N-acetylated foldamers having a C-terminal glycyl-phenylalanyl cyanomethyl ester, by a flexizyme. Foldamer–tRNA adducts can be used to initiate in vitro translation to form foldamer–peptide hybrids (mRNA, yellow; ribosome 50S, light blue; ribosome 30S, dark blue; amino acids, white circles). **d**, Monomeric units of **Q** with aspartate-like (red), ornithine-like (green) and tetraethylene glycol (TEG, blue) side chains, respectively. **e**, Foldamer substrates **1–11** used in this study (CME, cyanomethyl ester). **f**, Structure of a foldamer–peptide (GFKKKFDYKDDDDK) hybrid. The C-terminal peptide segment DYKDDDDK is a flag-tag sequence. Unless stated otherwise, DNA/mRNA encoding for this peptide sequence was used.

macrocyclization (for example through the stapling of side chains in α-helices[22] or by joining the ends of a sequence[12]) and conformational templates that initiate α-helicity[23,24]. Non-natural building blocks and cyclization have also been combined[25]. These conformationally restrained peptides generally perform better in the tight and selective recognition of biomolecules, as opposed to flexible sequences that must pay a higher entropic cost upon binding.

In contrast, some foldamers have folding properties that are superior to those of peptides, even peptides containing unnatural amino acids[26,27]. Aromatic oligoamide foldamers are in this class. Oligomers derived from 8-amino-2-quinolinecarboxylic acid[19] (henceforth referred to as **Q**, Fig. 1a) predictably form helical structures with remarkable stability, including in water[28,29]. For example, an octamer shows no denaturation at 120 °C in dimethylsulfoxide (DMSO)[19]. **Q** monomers are comparable to dipeptides in size (Fig. 1a), but, with their rigid aromatic structure, fewer rotatable bonds and a different pattern of hydrogen-bond donors and acceptors,

their sequences form distinctly non-proteinogenic helices with a diameter about twice as large as that of an α-helix (Fig. 1b). Like peptides, **Q** oligomers can be decorated with different side chains. However, quite unlike peptides, folding is a property of the backbone and is independent of the side chain. As a hint that robust folding of $\mathbf{Q}_n$ might be conferred to peptides, they have been shown to be stable enough to accommodate individual α-amino acids, the conformation of which is then dictated by the aromatic backbone[30,31]. We thus engaged in assessing the extent to which peptide–foldamer hybrid structures could be produced by ribosomal translation of mRNA and possibly exhibit synergistic folding properties.

Acylation of tRNA with foldamer substrates. Foldamer substrates were designed for attachment to tRNA, catalysed by the flexizyme 'eFx'. To ensure good yields, all substrates in this study included a C-terminal glycine spacer followed by a phenylalanine cyanomethylester (Gly-Phe-CME, Fig. 1c,e), which is an appropriate

Fig. 2 | In vitro translation of oligomeric foldamer–peptide/protein hybrids. a, Formulae of the expected targets (using substrates **1** and **4–10**). 'Peptide' refers to GFKKKFDYKDDDDK (shown in Fig. 1f). Dashed arrows represent the iterative exploration of foldamer sequences in this study. Red crosses indicate that the subsequent sequence was not translated (that is, from **5** and **9**). Thus, increasing the number of **Q** from 2 to 3 resulted in unsuccessful translation. Elongating (**PQ**)₂ by one **Q** also prevented translation. However, increasing the **P** content (using substrate **10**) allowed a pentameric foldamer–peptide hybrid to be formed. **b**, MALDI–TOF–MS spectra of foldamer–peptide products successfully formed using in vitro translation. From top to bottom: peptide initiated with **1** (red); initiation using **4** (red) and **6** (blue); initiation using **7** (blue); initiation using **8** (blue); and initiation using **10** (purple). No product could be observed for substrates **5** and **9**. **c**, MALDI–TOF–MS spectra (left) of a foldamer–protein hybrid formed using a DNA template for protein G (white, right). The major product corresponds to protein synthesis starting from the second (non-AUG) codon. C, calculated for [M+H]⁺; O, observed mass.

peptide donor for tRNA acylation mediated by eFx[5,32]. Three substrates were synthesized containing **Q** monomers with a range of side chains: aspartate-like (**1**), ornithine-like (**2**) and tetraethylene glycol (**3**) (Fig. 1d,e). Aminoacylation of these substrates was tested by charging onto an RNA microhelix, using an appropriate DMSO-containing reaction buffer (Supplementary Fig. 1). Note that this RNA microhelix was used as a tRNA mimic for reasons of detection simplicity, because its acylation can be readily quantified using band intensity on acid polyacrylamide gel electrophoresis (PAGE) and because it has been established that the yield of microhelix charging correlates with activity using tRNA[5]. The longer foldamers **4–11**, comprising several **Q** units with aspartate-like side chains and **P** units (6-aminomethyl-2-pyridinecarboxylic acid, Fig. 1a),

were also synthesized and could be charged onto the RNA microhelix (Supplementary Figs. 2–4), showing the high substrate tolerance of eFx. Because peptide synthesis in *Escherichia coli* is initiated with *N*-formyl methionine-charged tRNA$^{\text{fMet}}_{\text{CAU}}$, we carried out the acylation of in vitro transcript tRNA$^{\text{fMet}}_{\text{CAU}}$ by foldamer substrates **1–11** and examined their use in translation.

Scope of in vitro translation initiation with appended Qₙ oligomers. Initial experiments showed that foldamer–tRNA$^{\text{fMet}}_{\text{CAU}}$ from substrates **1–3**, containing **Q** monomers with variable side chains, could all initiate the synthesis of dodecapeptide KKKFDYKDDDDK (Fig. 1f). The expected foldamer–peptide hybrids were detectable by matrix-assisted laser desorption/ionization–time of flight mass

spectrometry (MALDI–TOF–MS) (Fig. 2a,b and Supplementary Fig. 1). The efficiencies of translation for these substrates were 10–20% that of formyl methionine-initiated translation (Supplementary Fig. 5). These yields are good considering that the substrates are substantially larger and more rigid than formyl methionine; they are comparable in size with the largest appendages previously used in peptide synthesis initiation[8,15,16,18,33,34]. Furthermore, initiation appears to work regardless of the side chain, and even a large tetraethylene glycol was accepted. Foldamer–tRNA$^{fMet}_{CAU}$ adducts containing two or three **Q** units with aspartate-like side chains were then tested in translation (from **4** and **5**, respectively; Fig. 2a). The initiation of peptide synthesis was possible using **4**, albeit with a lower yield than when using **1** (Supplementary Fig. 5), but no foldamer–peptide hybrid could be detected using **5** (Fig. 2a,b). To test whether delivery to the ribosome was preventing initiation with **5**, we increased the concentration of initiation factor 2 (IF2, a key protein in this process) from 0.4 to 8 µM, but the foldamer–peptide hybrid was not observed. **Q**$_n$ oligomers adopt compact helical structures[35] whose stability increases with oligomer length[19,36]. In these helices, five **Q** units span two helix turns. It is notable that foldamer **4** (**QQ**, 0.8 turns), and not **5** (**QQQ**, 1.2 turns), is acceptable to the ribosome—only the latter can form a full turn of helix. We also recognize that the narrowest point in the ribosome exit tunnel is ~ 1 nm in diameter[37], similar to the diameter of a folded **Q**$_n$ helix without side chains (Supplementary Fig. 6). It is therefore plausible that the helix of **5** will not pass this constriction if it cannot unfold.

Inclusion of pyridine-based monomers in Q$_n$ sequences. We sought to reduce the conformational stability of the foldamer helix to test whether it would permit translation of larger initiation units. This can be achieved by replacing **Q** with the more flexible **P** monomer (Fig. 1a). **P** has the same backbone atoms as **Q**, and sequences combining **P** and **Q** fold into similarly shaped helices[38,39]. However, **P** possesses a smaller surface for aromatic stacking and an additional rotatable bond at the methylene group that interrupts conjugation; thus, both factors should contribute to lowering the overwhelming stability of the **Q**$_n$ helices. For instance, **P**$_n$ oligomers do not fold[39]. In sequences **6–9**, **P** and **Q** units alternate (Fig. 1e). Using tRNA$^{fMet}_{CAU}$ acylated with these substrates, translation could be initiated with **6**, **7** and **8** (albeit with lower efficiency than with **1–3**) but not with the longest sequence **9** (Fig. 2a,b). As for **5**, increasing the concentration of IF2 from 0.4 to 8 µM brought no improvement. To find a foldamer with five aryl units suitable for translation, we produced a variant of **9** with an N-terminal **P** instead of **Q** (substrate **10**). The foldamer–tRNA$^{fMet}_{CAU}$ charged with **10** was accepted by the ribosome and could be used in translation initiation.

Substrate **10** is long enough to span two full aromatic helix turns and is equivalent to a dodecameric peptide in length. It constitutes the largest appendage to tRNA$^{fMet}_{CAU}$ and is the largest single block delivered to the ribosome that has been used to date. Translation with **7**, **8** and **10**, and not with **5** and **9**, may result from the smaller size of the **P** units, which lack a side chain and a main-chain aromatic ring. Alternatively, their higher flexibility might allow transient unfolding when required during translation, for example, to pass through the narrow constriction in the exit tunnel of the ribosome. However, one may also question whether the foldamer appendages have actually passed through the entire ribosome tunnel. The GFKKKFDYKDDDDK sequence formed in the above translation experiments is too short for the foldamer segment to protrude from the ribosomal exit tunnel before peptide synthesis is complete. Indeed, this would require 30–40 amino acids[40,41]. It is therefore possible that the foldamer–peptide hybrids are not fully traversing the exit tunnel, but are released after disassembly of the ribosome machinery.

To investigate the ability of these foldamers to navigate the exit tunnel, we used a longer mRNA template coding for protein G (74 amino acids, including a C-terminal flag-tag) and tRNA$^{fMet}_{CAU}$ loaded with substrates **6**, **8** and **10**. Foldamer–protein hybrids could be synthesized by the ribosome and correct product observed using MALDI–TOF–MS after translation (Fig. 2c and Supplementary Fig. 7). This observation clearly indicates that these foldamers are indeed passing entirely through the exit tunnel. It remains to be determined whether this reflects a broad tolerance of the ribosome tunnel for a range of non-peptidic substrates or whether aromatic foldamers happen to be a favourable case. Noteworthy is the concomitant presence of translated products lacking the foldamer initiators (Supplementary Fig. 7). It is possible that, after assembly of the ribosome–mRNA complex, dissociation of the large foldamer–tRNA$^{fMet}_{CAU}$ occurs, followed by the restart of translation at the second codon.

Solution studies of foldamer helices. To underpin our hypothesis on unfolding of foldamers in the ribosome exit tunnel, we investigated their conformation and stability in an aqueous environment. Foldamers **12–15** were synthesized, corresponding to initiators **7**, **5**, **8** and **9** lacking the C-terminal Phe-CME, respectively. Multidimensional NMR allowed for the complete assignment of their ^{1}H NMR spectra (Supplementary Figs. 10–13). Rotating-frame Overhauser spectroscopy (ROESY) experiments showed correlations indicating that all are helically folded (Supplementary Figs. 14–17). Although the patterns and intensities of the nuclear Overhauser effect (NOE) signals were not entirely identical, correlations between amide protons of adjacent residues were identified in all cases (Fig. 3a), consistent with the canonical quinoline helix in which amide protons reside at the inner rim (Fig. 3b)[39,42]. Other medium-range NOE signals between non-adjacent residues (i to $i+2$ or i to $i+3$) represent typical through-space correlations in quinoline helices where side chain, aromatic and Gly protons locate on the outer rim (Fig. 3b)[31,42]. The ^{1}H NMR spectra of **12–15** all featured at least one strongly upfield-shifted singlet near 6.4 ppm (Fig. 3e), corresponding to the H3 proton of the first aromatic ring starting from the C terminus (always a **Q**) that is shielded by the ring current effect of a stacked quinoline (the second quinoline ring from the C terminus) in the helical conformation[19].

Having established folding, we next investigated helix stability. NH/ND exchange rates allow for the assessment of exposure to the surrounding water and in part reflect conformational dynamics (Supplementary Figs. 18–21). The pseudo-first-order rate constants of amide NH/ND exchange in **12–15** could be calculated and were shown to be significantly lower for **13** and **15**. Within a given molecule, NH/ND exchange rates vary according to chemical nature and position in the sequence (Fig. 3d). When examining comparable functions, for example the terminal NH(Gly) of different oligomers, exchange was found to be faster for **12** and **14** than for **13** (Fig. 3c). The range of rates is considerable: the amide protons of **12**, except its NH(Gly), are quantitatively exchanged within 100 s, whereas the NH of the central **Q** of pentamer **15** exchanges with a half-life of 66 min (Supplementary Figs. 18 and 21). Overall, stability increases both with increasing length and on increasing the proportion of **Q**. Conformational stability may thus well be the factor that prevents translation initiation with **5** and **9**.

Conformational stability was also reflected in the ^{1}H NMR spectra. Helical conformations are inherently chiral, even if the molecules possess no stereogenic centres. As a result, CH_2 protons in **Q** (side chain) and **P** and Gly (main chain) are diastereotopic, and their signals may be anisochronous when exchange between left- and right-handed helices is slow on the NMR timescale[19], that is, when the helices have sufficient kinetic stability. Consistent with the higher stability of **13** and **15** revealed by NH/ND exchange rates, anisochronous CH_2 signals are obvious in the spectra of these
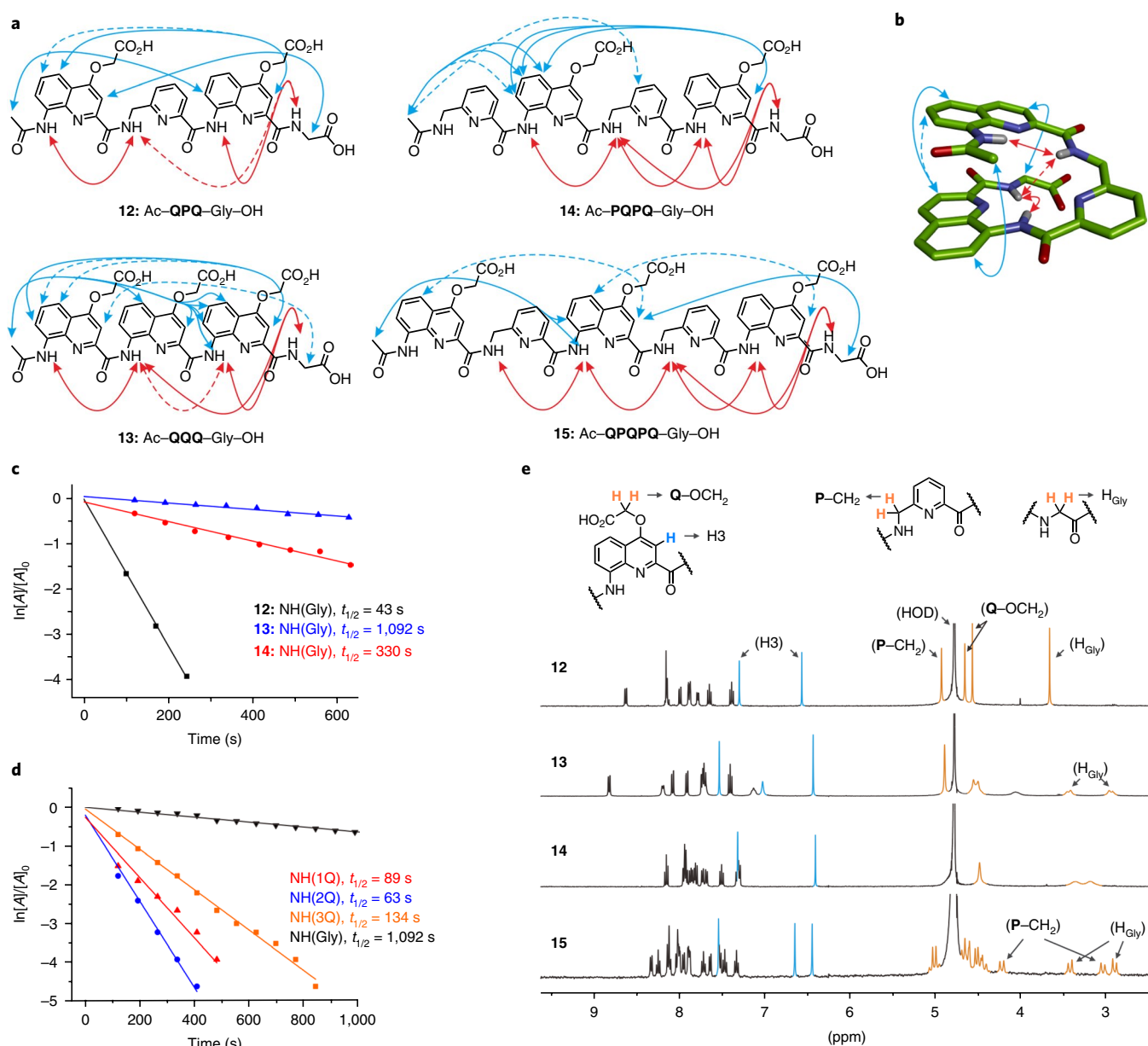
Fig. 3 | NMR studies of aromatic foldamer segments. a, Chemical formulae of aromatic foldamer segments used for solution-state conformation studies with identified NOEs in aqueous solution (9:1 H_2O/D_2O, 50 mM $NaHCO_3$). Red arrows indicate correlations between backbone amide protons. Blue arrows indicate correlations between sequentially non-adjacent residues. Solid and dashed arrows indicate strong and medium/weak interactions, respectively. **b**, Molecular model of **12** with observed NOEs. **c,d**, Pseudo-first-order rate plots of NH/ND exchange and half-life for NH(Gly) in D_2O at 25 °C of **12**, **13** and **14** (**c**) and amide protons of **13** (**d**). [A] and [A]$_0$ indicate the integrated peak area of amide protons at a given time and at $t = 0$, respectively. Monitoring of NH(Gly) of **15** was not possible due to signal overlap. **e**, Parts of ^{1}H NMR spectra of **12**, **13**, **14** and **15** in D_2O with 50 mM $NaHCO_3$ at 25 °C. Peaks in blue indicate H3 protons of quinoline rings. Peaks in orange indicate CH_2 protons of **Q** (side chain), **P** (main chain) and Gly (main chain) residues.

sequences, where multiple AB systems are present (Fig. 3e) that coalesced at elevated temperature (45 °C, Supplementary Figs. 23 and 25). In contrast, the diastereotopic protons appear as sharp averaged singlets in the spectrum of **12** as left- and right-handed helices exchange rapidly (Supplementary Fig. 22). The spectrum of **14** shows an intermediate situation with some broadening (Supplementary Fig. 24), suggesting that its dynamics, albeit faster than for **13** and **15**, are slower than for α-peptidic chains for which fast exchange on the NMR timescale is observed[43]. In summary, these results suggest that translation initiation occurs only when appended foldamer helices have a sufficient ability to transiently unfold to pass through the ribosome exit tunnel, and that this is

allowed for helices that are nevertheless more stable than a typical, isolated peptide helix.

Ribosomal synthesis of macrocyclic foldamer–peptide hybrids.
To further expand the chemical diversity produced by the ribosome and to exploit ribosomal uptake of helical foldamers with better defined conformations than short peptides, we endeavoured to express foldamer–peptide cyclic hybrids. In a macrocycle, the peptide and foldamer are attached at two points, which might result in a coupling of their respective conformations. Genetic code reprogramming with an N-terminal chloroacetyl (ClAc) amino acid allows for efficient macrocyclization through thioether formation
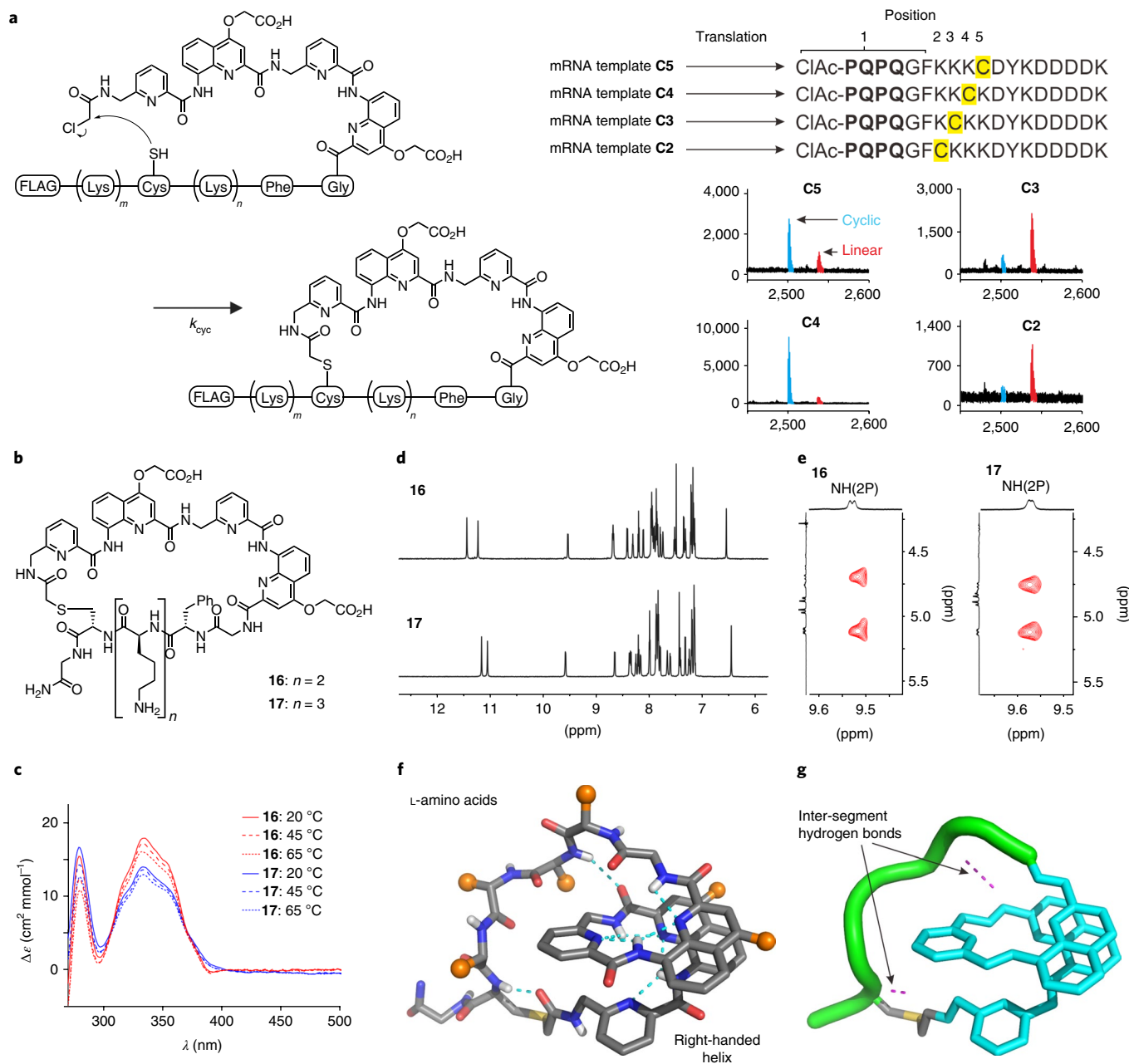
Fig. 4 | Macrocyclization of foldamer–peptide hybrids. a, Macrocyclization by thioether formation from an N-terminal chloroacetyl group and a cysteine thiol, and corresponding MALDI–TOF–MS spectra. **b**, Synthesized foldamer–peptide macrocycles. **c**, CD spectra of **16** and **17** in H_2O/DMSO-d_6 (7:3, vol/vol) at different temperatures. **d**, Selected parts of ^1H NMR spectra of **16** and **17** in H_2O/DMSO-d_6 (7:3, vol/vol) at 65 °C. **e**, Selected parts of TOCSY spectra of **16** and **17** in H_2O/DMSO-d_6 (7:3, vol/vol) at 65 °C showing NH–CH$_2$ J-couplings. **f**, Crystal structure of compound **17**. Side chains of lysine, phenylalanine and **Q** are shown as orange spheres. **g**, Stick–loop representation of the crystal structure of **17**. The peptide backbone (green loop) is held by the helical aromatic foldamer (cyan sticks). The thioether linkage is shown in yellow. TOCSY, total correlated spectroscopy.

with the thiol of a cysteine residue further along the sequence[12]. Precursor **11** (Fig. 1e) was prepared to include a terminal ClAc to form foldamer-containing macrocycles (Fig. 4a), and this substrate could initiate translation (Supplementary Fig. 4). Additional mRNA templates were designed to encode a cysteine either immediately after the foldamer initiator (template C2) or further along the peptide (templates C3, C4 and C5), and these were used for in vitro translation, initiated using **11**. Within 30 min of translation, cyclized species were detected as the major product for templates C4 and C5, whereas linear foldamer–peptide hybrids were still the major products for C2 and C3 (Fig. 4a). After 10 min translation, and release from the ribosome using EDTA, cyclization for C2

and C3 proceeded at a slower, similar rate ($k_{cyc} = 3 \times 10^{-4}\,s^{-1}$, Supplementary Figs. 8 and 9).

The effect of peptide stapling by a foldamer on macrocycle conformation was then investigated in solution. Macrocycles **16** and **17** were synthesized as analogues of cyclized translation products from C4 and C5 templates (Fig. 4b). Their circular dichroism (CD) spectra showed positive bands at 280 and 340 nm, indicating bias toward a right-handed foldamer helix[44] as a consequence of the L-chirality of the peptide. Heating had little effect on the CD spectra (Fig. 4c and Supplementary Figs. 26 and 27), hinting at helix stability even under harsh conditions such as 7:3 H_2O/DMSO (vol/vol) at 65 °C. ^1H NMR spectra of **16** and **17** showed poorly resolved signals at

room temperature (Supplementary Figs. 28 and 29), presumably due to nonspecific aggregation promoted by their amphipathic and zwitterionic nature. However, sharp spectra at 65 °C (Fig. 4d) allowed for the observation of quinoline H3 proton singlets near 6.4 ppm, indicating shielding by aromatic stacking. In addition, $NH-CH_2$ J^3-couplings of **P** units showed obvious diastereotopic patterns (Fig. 4e and Supplementary Figs. 30 and 31). Thus, the **PQPQ** segment in both **16** and **17** is helical, chirally biased, and stabilized with respect to non-cyclic sequence **14**. Helix conformation control by stereocentres can be remote[45]. Here, the nearest stereogenic centres are five atoms away from the foldamer helix at both C and N termini, which contrasts greatly with earlier examples of absolute handedness control[44].

Crystals of **17** could be obtained but diffracted only at 2.5 Å. The D-enantiomer of **17** was then also synthesized and mixed with L-**17** to produce a racemate. Crystals of racemic **17** diffracted at 0.9 Å, and the structure in the solid state could be resolved in centrosymmetrical space group $P\bar{1}$ (Supplementary Figs. 32 and 33). Two independent molecules in the asymmetric unit show essentially superimposable main-chain conformation, suggesting that this conformation is robust (Supplementary Fig. 34). The structure proved to be consistent with solution-phase observations (Fig. 4f,g and Supplementary Movie 1). The aromatic segment **PQPQ** of L-**17** is folded into a compact right-handed helix. Conversely, D-**17** is left-handed. The helical fold is similar to that of canonical Q_n helices. In contrast, the six-amino-acid peptide segment adopts a loop-like extended conformation. Two hydrogen bonds are established between two peptidic NH protons belonging to Lys2 and Cys5, and the two CO of the carbonyl-amino-methyl groups in position 6 of the two **P** units. These inter-segment interactions presumably mediate helix handedness control while restraining the peptide conformation. The peptide side chains are not involved, suggesting that the conformation may be sequence independent. The reciprocal conformational effects between these chemically distinct biotic and abiotic folded entities—a peptide and an aromatic oligoamide—are quite unique. The structure mirrors stapled helical peptides[22] in which the peptide is α-helical and the hydrocarbon staple is extended. Similar structures have also been observed in thioether-bridged macrocyclic peptides[46,47]. Such macrocycles were synthesized by the ribosome and were selected from large libraries to bind to a particular partner protein. When bound, these macrocycles use a helix to present a peptide loop for binding, with the helix involved to different degrees in the binding interface (Supplementary Fig. 35). This raises an attractive possibility of using the structures described here, helical foldamers presenting a peptide loop, for molecular recognition.

Conclusions

We have demonstrated that aromatic foldamer-appended peptides could be synthesized by the ribosome using genetic code reprogramming. Foldamer–tRNA prepared by flexizyme can be delivered as a single unit to the ribosome and successfully initiate peptide synthesis. The foldamers represent not only the largest single building blocks to be accepted by the ribosome, but also chemical entities very distinct from the peptide sequences that the ribosome has been optimized to accept by evolution. We find that translation requires a certain degree of conformational flexibility, possibly to allow for unfolding of the foldamer segments to pass through the ribosome exit tunnel. Yet, foldamers with folding propensities stronger than those of peptides of comparable sizes—a non-cyclic decapeptide rarely folds—are accepted for translation. It can be conceived that fine-tuning of folding–unfolding behaviour might allow translation of even larger appendages. In addition, macrocyclization chemistry was successfully applied to these foldamer–peptide hybrids. Helically folded aromatic foldamers in cyclic peptides act as a novel class of peptide linker that can serve as a structural scaffold to present the peptide in three-dimensional space. Solution and solid-state studies reveal a reciprocal influence of the peptide and foldamer helix conformations, presumably by mutual reduction of the entropy penalty inherent to folding. For this type of hybrid molecule, one may expect functional improvements for the peptide regions in terms of selectivity and binding affinity to target biomolecules. Conversely, the foldamer may be highly water-soluble and possess cell-penetrating properties[28]. An obvious subsequent step is to investigate the amenability of these constructs to sequence randomization and selection of functional species from libraries.

References

1. Fischer, N. et al. Structure of the *E. coli* ribosome–EF–Tu complex at <3 Å resolution by C_s-corrected cryo-EM. *Nature* **520**, 567–570 (2015).
2. Ernst, R. J. et al. Genetic code expansion in the mouse brain. *Nat. Chem. Biol.* **12**, 776–778 (2016).
3. Lajoie, M. J. et al. Genomically recoded organisms expand biological functions. *Science* **342**, 357–360 (2013).
4. Maini, R. et al. Ribosome-mediated incorporation of dipeptides and dipeptide analogues into proteins in vitro. *J. Am. Chem. Soc.* **137**, 11206–11209 (2015).
5. Murakami, H., Ohta, A., Ashigai, H. & Suga, H. A highly flexible tRNA acylation method for non-natural polypeptide synthesis. *Nat. Methods* **3**, 357–359 (2006).
6. Hartman, M. C., Josephson, K., Lin, C. W. & Szostak, J. W. An expanded set of amino acid analogs for the ribosomal translation of unnatural peptides. *PLoS One* **2**, e972 (2007).
7. Shimizu, Y. et al. Cell-free translation reconstituted with purified components. *Nat. Biotechnol.* **19**, 751–755 (2001).
8. Rogers, J. M. & Suga, H. Discovering functional, non-proteinogenic amino acid containing, peptides using genetic code reprogramming. *Org. Biomol. Chem.* **13**, 9353–9363 (2015).
9. Katoh, T., Tajima, K. & Suga, H. Consecutive elongation of D-amino acids in translation. *Cell Chem. Biol.* **24**, 46–54 (2017).
10. Fujino, T., Goto, Y., Suga, H. & Murakami, H. Reevaluation of the D-amino acid compatibility with the elongation event in translation. *J. Am. Chem. Soc.* **135**, 1830–1837 (2013).
11. Fujino, T., Goto, Y., Suga, H. & Murakami, H. Ribosomal synthesis of peptides with multiple β-amino acids. *J. Am. Chem. Soc.* **138**, 1962–1969 (2016).
12. Goto, Y. et al. Reprogramming the translation initiation for the synthesis of physiologically stable cyclic peptides. *ACS Chem. Biol.* **3**, 120–129 (2008).
13. Ohta, A., Murakami, H., Higashimura, E. & Suga, H. Synthesis of polyester by means of genetic code reprogramming. *Chem. Biol.* **14**, 1315–1322 (2007).
14. Kawakami, T., Murakami, H. & Suga, H. Ribosomal synthesis of polypeptides and peptoid–peptide hybrids. *J. Am. Chem. Soc.* **130**, 16861–16863 (2008).
15. Goto, Y. & Suga, H. Translation initiation with initiator tRNA charged with exotic peptides. *J. Am. Chem. Soc.* **131**, 5040–5041 (2009).
16. Torikai, K. & Suga, H. Ribosomal synthesis of an amphotericin-B inspired macrocycle. *J. Am. Chem. Soc.* **136**, 17359–17361 (2014).
17. Passioura, T. & Suga, H. A RaPID way to discover nonstandard macrocyclic peptide modulators of drug targets. *Chem. Commun.* **53**, 1931–1940 (2017).
18. Terasaka, N., Hayashi, G., Katoh, T. & Suga, H. An orthogonal ribosome–tRNA pair via engineering of the peptidyl transferase center. *Nat. Chem. Biol.* **10**, 555–557 (2014).
19. Jiang, H., Léger, J. M. & Huc, I. Aromatic δ-peptides. *J. Am. Chem. Soc.* **125**, 3448–3449 (2003).
20. Boersma, M. D. et al. Evaluation of diverse α/β-backbone patterns for functional α-helix mimicry: analogues of the Bim BH3 domain. *J. Am. Chem. Soc.* **134**, 315–323 (2012).
21. Fuller, A. A. et al. Evaluating β-turn mimics as β-sheet folding nucleators. *Proc. Natl Acad. Sci. USA* **106**, 11067–11072 (2009).

22. Walensky, L. D. & Bird, G. H. Hydrocarbon-stapled peptides: principles, practice, and progress. *J. Med. Chem.* **57**, 6275–6288 (2014).
23. Lao, B. B. et al. In vivo modulation of hypoxia-inducible signaling by topographical helix mimetics. *Proc. Natl Acad. Sci. USA* **111**, 7531–7536 (2014).
24. Fremaux, J. et al. α-Peptide-oligourea chimeras: stabilization of short α-helices by non-peptide helical foldamers. *Angew. Chem. Int. Ed.* **54**, 9816–9820 (2015).
25. Cheng, P. N. & Nowick, J. S. Giant macrolactams based on β-sheet peptides. *J. Org. Chem.* **76**, 3166–3173 (2011).
26. Goodman, C. M., Choi, S., Shandler, S. & DeGrado, W. F. Foldamers as versatile frameworks for the design and evolution of function. *Nat. Chem. Biol.* **3**, 252–262 (2007).
27. Guichard, G. & Huc, I. Synthetic foldamers. *Chem. Commun.* **47**, 5933–5941 (2011).
28. Gillies, E. R., Deiss, F., Staedel, C., Schmitter, J. M. & Huc, I. Development and biological assessment of fully water-soluble helical aromatic amide foldamers. *Angew. Chem. Int. Ed.* **46**, 4081–4084 (2007).
29. Delaurière, L. et al. Deciphering aromatic oligoamide foldamer–DNA interactions. *Angew. Chem. Int. Ed.* **51**, 473–477 (2012).
30. Kudo, M., Maurizot, V., Kauffmann, B., Tanatani, A. & Huc, I. Folding of a linear array of α-amino acids within a helical aromatic oligoamide frame. *J. Am. Chem. Soc.* **135**, 9628–9631 (2013).
31. Hu, X., Dawson, S. J., Nagaoka, Y., Tanatani, A. & Huc, I. Solid-phase synthesis of water-soluble helically folded hybrid α-amino acid/quinoline oligoamides. *J. Org. Chem.* **81**, 1137–1150 (2016).
32. Saito, H., Kourouklis, D. & Suga, H. An in vitro evolved precursor tRNA with aminoacylation activity. *EMBO J.* **20**, 1797–1806 (2001).
33. Goto, Y., Ashigai, H., Sako, Y., Murakami, H. & Suga, H. Translation initiation by using various N-acylaminoacyl tRNAs. *Nucleic Acids Symp. Ser.* **50**, 293–294 (2006).
34. Goto, Y., Murakami, H. & Suga, H. Initiating translation with D-amino acids. *RNA* **14**, 1390–1398 (2008).
35. Qi, T. et al. Solvent dependence of helix stability in aromatic oligoamide foldamers. *Chem. Commun.* **48**, 6337–6339 (2012).
36. Delsuc, N. et al. Kinetics of helix-handedness inversion: folding and unfolding in aromatic amide oligomers. *ChemPhysChem* **9**, 1882–1890 (2008).
37. Voss, N. R., Gerstein, M., Steitz, T. A. & Moore, P. B. The geometry of the ribosomal polypeptide exit tunnel. *J. Mol. Biol.* **360**, 893–906 (2006).
38. Sánchez-García, D. et al. Nanosized hybrid oligoamide foldamers: aromatic templates for the folding of multiple aliphatic units. *J. Am. Chem. Soc.* **131**, 8642–8648 (2009).
39. Baptiste, B., Douat-Casassus, C., Laxmi-Reddy, K., Godde, F. & Huc, I. Solid phase synthesis of aromatic oligoamides: application to helical water-soluble foldamers. *J. Org. Chem.* **75**, 7175–7185 (2010).
40. Cabrita, L. D. et al. A structural ensemble of a ribosome–nascent chain complex during cotranslational protein folding. *Nat. Struct. Mol. Biol.* **23**, 278–285 (2016).
41. Nilsson, O. B. et al. Cotranslational protein folding inside the ribosome exit tunnel. *Cell. Rep.* **12**, 1533–1540 (2015).
42. Dolain, C. et al. Solution structure of quinoline- and pyridine-derived oligoamide foldamers. *Chemistry* **11**, 6135–6144 (2005).
43. Solà, J., Helliwell, M. & Clayden, J. N- versus C-terminal control over the screw-sense preference of the configurationally achiral, conformationally helical peptide motif Aib$_8$GlyAib$_8$. *J. Am. Chem. Soc.* **132**, 4548–4549 (2010).
44. Kendhale, A. M. et al. Absolute control of helical handedness in quinoline oligoamides. *J. Org. Chem.* **76**, 195–200 (2011).
45. Li, J. et al. An in-tether sulfoxide chiral center influences the biophysical properties of the N-capped peptides. *Bioorg. Med. Chem.* **25**, 1756–1761 (2017).
46. Kodan, A. et al. Structural basis for gating mechanisms of a eukaryotic P-glycoprotein homolog. *Proc. Natl Acad. Sci. USA* **111**, 4049–4054 (2014).
47. Yu, H. et al. Macrocycle peptides delineate locked-open inhibition mechanism for microorganism phosphoglycerate mutases. *Nat. Commun.* **8**, 14932 (2017).
48. Gillies, E. R., Dolain, C., Léger, J. M. & Huc, I. Amphipathic helices from aromatic amino acid oligomers. *J. Org. Chem.* **71**, 7931–7939 (2006).

Acknowledgements

Author contributions

S.K. and J.M.R. contributed equally to this work. S.K. and S.J.D. synthesized new compounds. S.K. carried out solution conformational studies. J.M.R. performed in vitro aminoacylation and translation experiments. P.K.M. carried out crystallographic studies. All authors contributed to designing the research, to discussing the results and to writing the manuscript.

Competing interests

The authors declare no competing interests.

Additional information

Supplementary information is available for this paper at https://doi.org/10.1038/s41557-018-0007-x.

Reprints and permissions information is available at www.nature.com/reprints.

Correspondence and requests for materials should be addressed to H.S. or I.H.

Publisher's note: Springer Nature remains neutral with regard to jurisdictional claims in published maps and institutional affiliations.